

SANPO

A Scene Understanding, Accessibility and Human Navigation Dataset

Sagar M. Waghmare* Kimberly Wilber*[†] Dave Hawkey* Xuan Yang* Matthew Wilson*

Stephanie Debats* Cattalyya Nuengsigkapan* Astuti Sharma* Lars Pandikow*[‡]

Huisheng Wang* Hartwig Adam* Mikhail Sirotenko*

Abstract

Vision is essential for human navigation. The World Health Organization (WHO) estimates that 43.3 million people were blind in 2020, and this number is projected to reach 61 million by 2050. Modern scene understanding models could empower these people by assisting them with navigation, obstacle avoidance and visual recognition capabilities. The research community needs high quality datasets for both training and evaluation to build these systems. While datasets for autonomous vehicles are abundant, there is a critical gap in datasets tailored for outdoor human navigation. This gap poses a major obstacle to the development of computer vision based Assistive Technologies. To overcome this obstacle, we present SANPO, a large-scale egocentric video dataset designed for dense prediction in outdoor human navigation environments. SANPO contains 701 stereo videos of 30+ seconds captured in diverse real-world outdoor environments across four geographic locations in the USA. Every frame has a high resolution depth map and 112K frames were annotated with temporally consistent dense video panoptic segmentation labels. The dataset also includes 1961 high-quality synthetic videos with pixel accurate depth and panoptic segmentation annotations to balance the noisy real world annotations with the high precision synthetic annotations.

SANPO is already publicly available and is being used by mobile applications like Project Guideline to train mobile models that help low-vision users go running outdoors independently. To preserve anonymization during peer review, we will provide a link to our dataset upon acceptance.

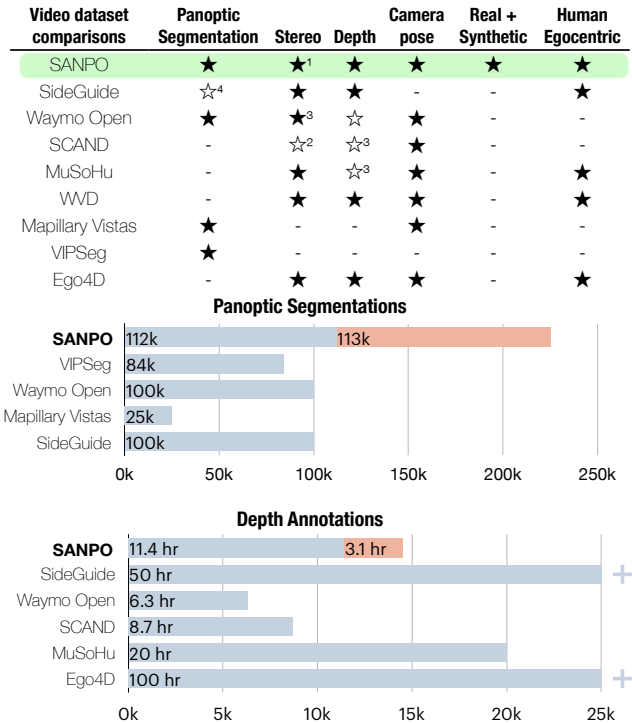


Figure 1. **SANPO** is the only human-egocentric dataset with panoptic masks, multi-view stereo, depth, camera pose, and both real and synthetic data. SANPO has the largest number of panoptic frames among related work and a respectable number of depth annotations. (Note: ¹: multi-view, ²: partial coverage, ³: sparse depth, ⁴: sparse segmentation)

1. Introduction

An estimated 295 million people worldwide experience moderate to severe visual impairment [4]. Advances in human navigation systems [22] could significantly improve

*Google Research [†]Work done while at Google [‡]Parallel Domain

their quality of life. To realize this potential, AI systems require robust egocentric scene understanding. Building this capability depends on the availability of large-scale, high-quality, and diverse datasets. The past decade has seen a surge in datasets for autonomous driving [19, 29, 30, 45]. However, these datasets are not suitable for the unique challenges of egocentric human navigation because they are designed for self-driving vehicles. These challenges include unusual viewpoints, motion artifacts, and dynamic human-object interactions. Unlike cars, which primarily operate in structured environments, humans navigate spaces that are often cluttered, unpredictable, and less regulated. This critical lack of publicly available human navigation-specific datasets hinders the development of robust assistive technologies.

To address this, we present SANPO, a comprehensive dataset designed to support research on outdoor human egocentric scene understanding. SANPO offers a rich combination of real and synthetic data. It is comprised of two underlying datasets: **SANPO-Real** contains 617K stereo video frame pairs with 617K estimated depth maps and 112K dense video panoptic masks. **SANPO-Synthetic** contains 113K video frames with pixel-accurate depth maps and dense video panoptic masks.

SANPO’s diversity and complexity also makes it an invaluable resource for advancing dense prediction tasks beyond human navigation. The inclusion of two stereo camera videos for each real session offers further potential for advancing multi-view methods.

2. Related Work

We can categorize the relevant scene understanding datasets into four categories: (i) Accessibility and Human Navigation, (ii) Human Egocentric, (iii) Autonomous Driving, and (iv) General Scene Understanding. See A.2.2 in the supplementary material for a comparison of many contemporary datasets.

2.1. Accessibility and Human Navigation

Few datasets in the literature explore accessibility and human navigation [1, 33, 35, 47], with SideGuide [35] standing out as the most relevant and extensive example. While both SANPO and SideGuide share a focus on egocentric human navigation, SANPO differentiates itself through several key advantages: i) Scale and Diversity: SANPO-Real surpasses SideGuide with a significantly larger dataset (617K stereo pairs vs. 180K) and broader environmental diversity, spanning urban, suburban, parks, trails, open terrain, etc. compared to SideGuide’s focus on urban sidewalks. ii) Temporally Consistent Video Segmentation Annotation: SANPO provides dense, temporally consistent video panoptic segmentation annotations, whereas, SideGuide offers sparse object masks. iii) Depth Labels: While both datasets provide estimated depth labels, SANPO utilizes CREStereo [24]

for potentially higher accuracy. iv) Synthetic Counterpart: SANPO includes a synthetic counterpart designed specifically to empower synthetic-to-real domain adaptation research.

2.2. Human Egocentric

Several datasets provide relevant data from a human egocentric perspective. SCAND [20], designed for robot navigation, includes depth and odometry labels but lacks the semantic segmentation crucial for scene understanding in human navigation. MuSoHu [34], captured with various sensors including a stereo camera, LIDAR, microphone array, and a 360-degree camera, offers depth and odometry labels while exhibiting motion artifacts typical of human movement. However, it also lacks semantic segmentation labels. Ego4D [13] is a large-scale dataset, but its focus extends beyond human navigation, and it lacks the necessary semantic segmentation for this task.

On the synthetic front, MOTSynth [11] and WVD [31] offer limited relevance. MOTSynth, while including segmentation and depth annotations, is limited by its focus on pedestrian-only annotations and restricted egocentric views. WVD, designed for violence detection, lacks both segmentation and depth labels essential for understanding the navigation environment.

2.3. Autonomous Driving

Datasets for autonomous vehicles, such as Cityscapes [9, 39], Argoverse [45], Waymo [30], and CamVid [5], among others [7, 26, 29, 38, 41], are prevalent in the field of computer vision. While these datasets often include rich annotations like stereo video, segmentation, depth, and 3D object detection labels, they prioritize vehicle-centric perception. Though there are several such datasets, they are not sufficient to address the unique challenges posed by human navigation environments. Egocentric environments often feature unstructured, unpredictable, and cluttered scenes, with unusual viewpoints, and motion artifacts due to human movement. They also exhibit dynamic human-object interactions. Addressing these challenges requires specialized datasets tailored to human navigation scenarios.

2.4. General-Purpose Scene Understanding

Datasets such as MSCOCO [27], DAVIS-2017 [6], and YouTube-VOS [46] focus on object detection and segmentation. Similar to autonomous driving datasets, they offer rich annotations but lack the attributes required for building a human navigation system.

Overall, existing datasets, though plentiful, don’t adequately satisfy the requirements of human navigation in diverse environments. See A.2.2 in the supplementary material for a broad comparison.

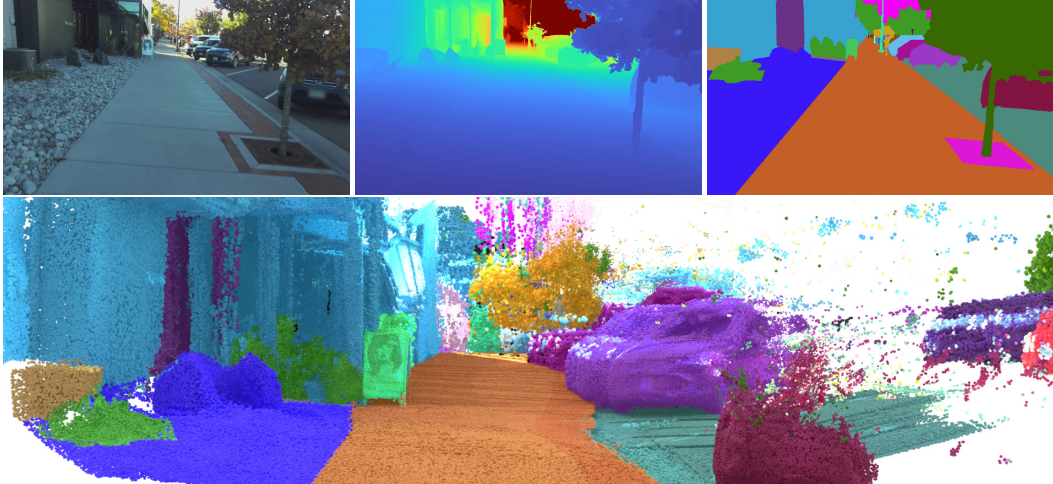


Figure 2. **SANPO Real Sample.** Top row shows a stereo left frame from a session along with its metric depth and segmentation annotations. Bottom row shows the 3D scene of the session built using the annotations we provide. Points from several seconds of video are accumulated and aligned with ICP.

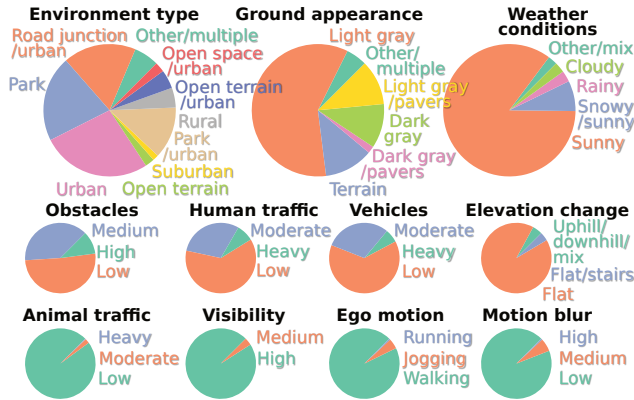


Figure 3. **SANPO-Real environment diversity**, showing the distribution of video-level annotations for 11 of the 12 attributes. Each pie chart shows that annotation over all 701 sessions.

3. SANPO

SANPO is comprised of *SANPO-Real*, a collection captured by real-world volunteer runners, and *SANPO-Synthetic*, a “digital twin” recreation in a virtual environment. In this section, we provide a detailed overview of both.

3.1. SANPO-Real

3.1.1 Data Collection

Collection Statistics SANPO-Real consists of 701 sessions recorded simultaneously with two stereo cameras, yielding four RGB video streams per session. Each video is approximately 30 seconds long, captured at 15 frames per second (FPS). We provide all videos in a lossless format to support stereo vision research, with 597 sessions at a resolution of

2208×1242 pixels and the remainder at 1920×1080 pixels. All videos were rectified using ZED software. In total, we collected 617,408 stereo frames. The chest-mounted ZED-2i, equipped with a 4mm lens, captured 308,957 stereo frames. This setup provided long-range depth from a stable mounting point, minimizing motion blur. The lightweight head-mounted ZED-M contributed 308,451 stereo frames, offering a wide field of view for comprehensive video.

Camera rig To accommodate SANPO-Real’s multi stereo camera requirements, we designed a specialized data collection rig for our volunteer runners to wear. Please see [A.1.1](#) in the supplementary material to learn more about it.

Ethics, Diversity and Privacy A dedicated team of volunteers employed at our company meticulously collected data. To ensure integrity, we provided clear guidelines on where and how to collect data, and strictly adhered to all relevant local, state, and city laws.

We collected data across four diverse US locations: San Francisco CA, Mountain View CA, Boulder CO, and NYC. These regions span urban areas, suburbs, city streets, and public parks. Our volunteers captured data under a wide range of conditions within each region, varying weather (including snow and rain), different times of day, and diverse ground types. They also navigated obstacles, varied their speeds, and encountered varying levels of traffic.

First, each volunteer reviewed their collected samples, immediately deleting any that didn’t meet our guidelines. Next, all the remaining videos were processed to remove personally identifiable information (PII), specifically faces and license plates ¹. Finally, only after completing these

¹ We computed depth annotations before blurring PII, as blurry patches can lead to inaccurate results.

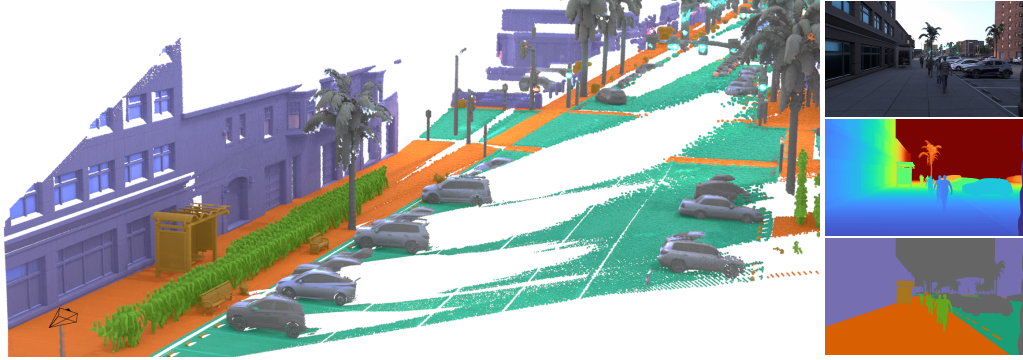


Figure 4. **SANPO-Synthetic Sample.** Right column shows a single frame from a synthetic session along with its metric depth and segmentation annotation. Left column shows the 3D scene of the session built using the annotations. Points come from the accumulated depth maps and camera locations across many frames.

privacy measures did we upload the videos to our cloud storage.

3.1.2 Annotation

Each session includes session-level attributes such as human traffic, density of obstacles, environment type *etc.*, 12 in total. The distribution of these annotations in Fig. 3 showcases the diversity of environments present in SANPO-Real. Additionally, we provide camera poses for every stereo recording derived from fused IMU and VIO measurements provided by the ZED software. Finally, we provide depth and panoptic segmentation annotations.

Depth For each stereo video we provide a sparse depth map generated by the ZED SDK and, similar to SideGuide [35], a dense depth map estimated using a stereo algorithm. We use CREStereo [24], a state-of-the-art ML-based stereo depth model. CREStereo maps stereo frames to a disparity map, which we convert to depth using camera intrinsics and limit the range to 0-80 meters. These depth maps have resolution of 1280×720 pixels, a result of CREStereo’s architecture.

Temporally Consistent Panoptic Segmentation We developed a segmentation taxonomy specifically for egocentric human navigation. This taxonomy balances panoptic segmentation with the need for detailed analysis of the navigation environment. It includes 31 categories: 15 “*thing*” classes (distinguishable objects) and 16 “*stuff*” classes (amorphous regions). A detailed taxonomy is provided in A.3.2 in the supplementary material. Using this taxonomy we provide panoptic segmentation annotations for 237 sessions. We annotated the left stereo video from one camera within each session, resulting in annotations for 146 videos captured by the long-range ZED-2i camera and 91 videos captured by the wide-angle ZED-M camera. All annotations are temporally consistent, ensuring that each object maintains a unique ID throughout the video. SANPO-Real offers a combination

of human-annotated and machine-propagated annotations. 18,787 human-annotated and 93,981 machine-propagated frames. A total of 975,207 object mask, with 195,187 manually segmented and 780,020 machine propagated. Section A.3.3 in the supplementary material details the annotation process. Figure 2 provides a visual example of a SANPO-Real session.

3.2. SANPO-Synthetic

The high cost of building large-scale real-world datasets [36, 40] creates significant interest in synthetic-to-real domain adaptation research [36, 40]. To support this research and complement SANPO-Real, we partnered with *Parallel Domain* to generate high-quality synthetic data. We worked closely with *Parallel Domain* to define simulation environments, providing detailed specifications and distributions for various simulation entities. The synthetic environment was optimized to replicate real-world capture conditions, including scenery, camera parameters, object placement and frequency. Through an iterative process, we achieved a synthetic dataset that closely matches SANPO-Real. Please see section A.2.1 in the supplementary material for full specifications of the rendering environment (camera intrinsics, obstacle distribution, *etc.*)

3.2.1 Simulation Statistics and Annotations

SANPO-Synthetic comprises 113,794 annotated monocular video frames from 1961 rendered sessions, simulating real-world camera configurations. To achieve this, 960 sessions utilize a (simulated) chest-level ZED-2i, while 1001 sessions employ a head-mounted ZED-M, with parameters mirroring their physical counterparts. This dataset features diverse frame rates of 5, 14.28, and 33.33 FPS.

Each synthetic video is accompanied by camera pose trajectories, dense depth maps and temporally consistent panoptic segmentation masks. A key attribute of SANPO-

Synthetic is its pixel-perfect annotations. Figure 4 provides a visual example of a SANPO-Synthetic session.

4. Analysis

SANPO offers a comprehensive dataset of 2662 sessions, encompassing 701 real sessions (“SANPO-Real”) captured across diverse real-world environments and conditions, and 1961 synthetic sessions (“SANPO-Synthetic”) meticulously simulated with varying distributions of simulation entities.

Data Diversity Figure 6 demonstrates the breadth of SANPO’s data diversity by showcasing real samples across various weather conditions and human traffic levels, categorized based on session-level attributes’ annotation. These session-level attributes could potentially be used to create views of SANPO to satisfy applications’ data requirements.

Distribution of Semantic Labels and Instances Figure 5 illustrates the distribution of semantic labels as a percentage of images containing them. Common human navigation specific labels like Building, Obstacle, Pole, Tree, Curb, Sidewalk, *etc.* are more prevalent. The quantity of annotated objects across the dataset is shown in Figure 7. The density of pedestrians is shown in the supplementary material; see Fig. 11 in A.2.3. Due to the controlled nature of virtual environments—where each object is masked including the objects distant from the egoperson—SANPO-Synthetic exhibits a considerably higher number of instances compared to SANPO-Real.

Depth Distribution Figure 8 shows the depth distribution of annotated objects within the dataset, revealing a contrast between SANPO-Real and SANPO-Synthetic. Both datasets have many annotated objects further than 20m away, but the distribution of SANPO-Synthetic skews much further than SANPO-Real. This is because the synthetic rendering pipeline can generate segmentations for objects that are arbitrarily far away.

5. Benchmarks

In this section, we establish baselines for SANPO dataset in two distinct evaluation settings: 1) **Zero-Shot Evaluation:** We assess the ability of published model checkpoints to generalize directly to the SANPO dataset. 2) **SANPO Benchmark:** We establish baselines for state-of-the-art architectures on dense prediction tasks using the SANPO dataset. Please see A.4.2 in the supplementary material for detailed experimental setup.

Metrics We evaluate the models’ performance using the following well established metrics:

- Semantic Segmentation: Mean Intersection over Union (mIoU) as in [50].

- Panoptic Segmentation: Panoptic Quality (PQ) as in [50].
- Depth Estimation: Fraction of depth inliers across the depth map, $\mathbb{E} \left[\max\left(\frac{y}{y'}, \frac{y'}{y}\right) \leq 1.25 \right]$, denoted as $\delta_{\leq 1.25}$, as in [3].

We report metrics on the test set of SANPO-Real. For semantic and panoptic segmentation, metrics are reported only on the human-annotated subset of the SANPO-Real test set.

5.1. Zero-Shot Evaluation

Our goal with SANPO is to provide a dataset representative of outdoor human navigation tasks from an egocentric perspective, which is distinct from domains like autonomous driving. This evaluation establishes zero-shot baselines and assesses the dataset’s challenge for zero-shot prediction.

Semantic Segmentation Baseline For this baseline we used the state-of-the-art Kmax-Deeplab [50] trained on the Cityscapes dataset [9]. For a fair comparison, we mapped the Cityscapes taxonomy to SANPO taxonomy, excluding 18 SANPO classes that lack direct mapping. We do not report panoptic quality for this baseline due to mismatch in “thing” classes of the Cityscapes and SANPO. For details on the Cityscapes to SANPO taxonomy mapping please refer to A.4.1 in the supplementary material.

Depth Estimation Baseline For this baseline, we used the publicly available checkpoint for ZoeDepth-M12 NK [3].

Foundation Models Baseline We also evaluated two foundation models: 1) **Segment Anything Model (SAM) [21]**, using the center point prompt and reporting instance-level mIoU for interactive segmentation tasks [43]. We excluded instances smaller than 2% of the image size for evaluation efficiency. 2) **Depth-Anything [48]**, using their outdoor metric depth model.

Our findings (Table 1) highlight the challenge SANPO presents for depth and segmentation models. Despite their focus on metric depth estimation and zero-shot transfer, ZoeDepth [3] and Depth-Anything [48] demonstrate limited performance on SANPO-Real with $\delta_{\leq 1.25}$ scores of 0.135 and 0.22, respectively. This underscores the need for more diverse metric depth datasets to improve generalization. Similarly, for segmentation, Kmax-Deeplab (ConvNeXt-L) exhibits a dramatic performance drop from its 83.5 mIoU on Cityscapes to 42.4 on SANPO-Real (using human-annotated ground truth only). This demonstrates that SANPO is generally a quite challenging dataset for current state-of-the-art segmentation methods.

5.2. SANPO Benchmark

We establish training baselines on SANPO using state-of-the-art architectures: Kmax-Deeplab [50] for panoptic

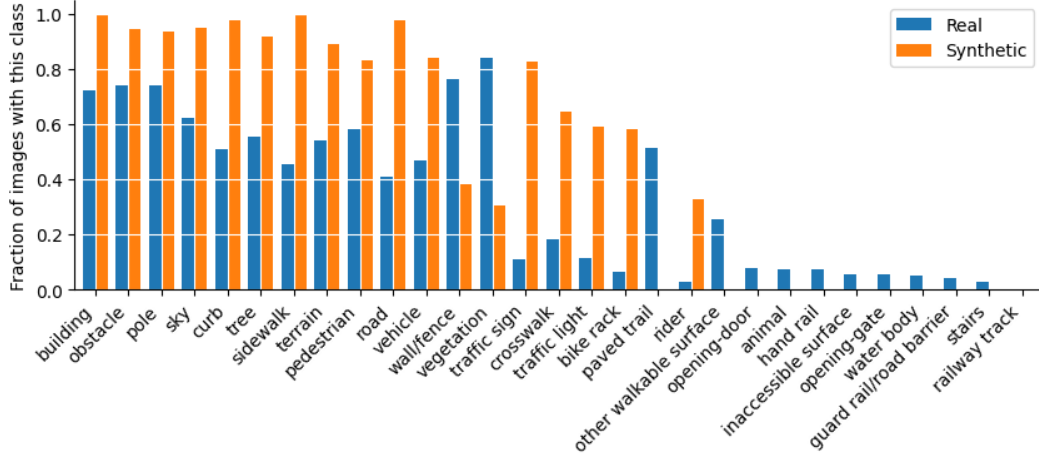


Figure 5. **Semantic label occurrences in SANPO:** Common human navigation specific labels like Building, Obstacle, Pole, Tree, Curb, Sidewalk etc. feature more prominently.

Pretrained Semantic Segmentation Model on Cityscape [9]				
Method	Encoder	mIoU \uparrow SANPO-Real	mIoU \uparrow Cityscapes [9]	
Kmax-Deeplab [50]	ResNet-50 [16]	38.6	79.7	
Kmax-Deeplab [50]	ConvNeXt-L [28]	42.4	83.5	
Segmentation Foundation Model				
Method	Model	Instance mIoU \uparrow SANPO-Real	Instance mIoU \uparrow Cityscapes [9]	
Center Point Prompt [21]	SAM [21]	48.9	41.0	
Pretrained Depth Estimation Model				
Method	Encoder	$\delta_{\leq 1.25} \uparrow$ SANPO-Real	$\delta_{\leq 1.25} \uparrow$ KITTI [12]	$\delta_{\leq 1.25} \uparrow$ Cityscapes-DVPS [39]
ZoeDepth [3]	BEiT ₃₈₄ -L [2]	0.135	0.97	0.39
Depth Foundation Model				
Method	Model	$\delta_{\leq 1.25} \uparrow$ SANPO-Real	$\delta_{\leq 1.25} \uparrow$ KITTI [12]	$\delta_{\leq 1.25} \uparrow$ Cityscapes-DVPS [39]
Metric Depth	Depth-Anything [48]	0.22	0.98	0.57

Table 1. **SANPO is a Challenging Dataset.** Zero-shot performance of various pre-trained models on the SANPO-Real test set. Higher values indicate better performance across all metrics.

segmentation and BinsFormer [25] for depth estimation. Table 2 presents the baseline performance of these models, trained on SANPO-Train and evaluated on SANPO-Real-Test. Only the human annotated subset of SANPO-Real-Test was used for evaluating panoptic segmentation.

Panoptic Segmentation The results on SANPO (mIoU ranging from 40.0 to 48.1) fall significantly below those achieved on Cityscapes (mIoU ranging from 79.7 to 83.5).

This disparity underscores the increased difficulty of the SANPO dataset, likely attributable to its substantially larger scale and greater diversity.

Depth Estimation The BinsFormer architecture demonstrates a notable performance gap between KITTI and SANPO-Real. While achieving an impressive $\delta_{\leq 1.25}$ of 0.96 on KITTI [12, 25], the same architecture—BinsFormer with a Resnet-50 backbone—only reaches a $\delta_{\leq 1.25}$ of 0.45



Figure 6. **SANPO is a Diverse Dataset.** An example of SANPO’s data diversity across weather conditions (left) and human traffic levels (right) based on the session-level attributes’ annotation. Please zoom in for better view.

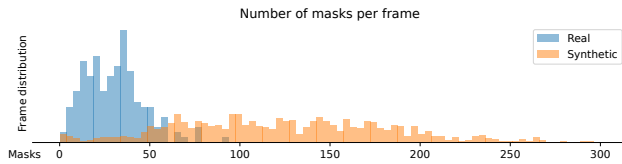


Figure 7. **Mask Quantity in SANPO.** A normalized histogram of “object” counts in SANPO, where “objects” are connected components of each unique panoptic label covering at least 100px. Real-world images typically have fewer annotated instances per image, rarely exceeding 40. In contrast, synthetic images feature significantly higher instance density, reflecting the controlled nature of virtual environments where each object can be individually masked.

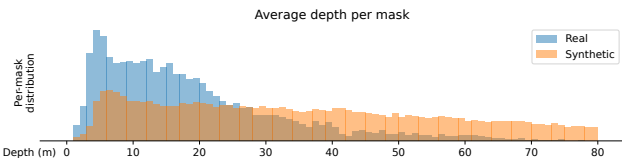


Figure 8. **SANPO Depth Distribution.** A normalized histogram of the average depth of each annotated object in SANPO-Real and SANPO-Synthetic, where “annotated objects” are connected components of each unique panoptic label covering at least 100px. Objects in SANPO-Synthetic tend to be further away than SANPO-Real because of the pixel-perfect segmentation and depth groundtruth. In both datasets, there are many objects further than 20m away, creating interesting challenges for obstacle detection applications.

on SANPO-Real. This significant difference emphasizes the value of SANPO as a challenging benchmark for driving progress in depth estimation research.

We also investigated two key aspects of the SANPO dataset for panoptic segmentation:

Machine-Propagated Annotations Table 3 shows that restricting training to human-annotated ground truth has minimal impact on performance, validating the accuracy of SANPO’s machine-propagated annotations. See A.3.3 in the supplementary material for an additional detailed quantitative analysis.

Panoptic Segmentation : Kmax-DeepLab [50]			
Dataset	Encoder	mIoU \uparrow	PQ \uparrow
SANPO-Synthetic-Train	Resnet-50 [16]	14.6	9.6
SANPO-Real-Train	Resnet-50 [16]	43.4	34.6
SANPO-Synthetic-Train	ConvNeXt-L [28]	17.6	11.1
SANPO-Real-Train	ConvNeXt-L [28]	46.0	38.4
Depth Estimation : BinsFormer [25]			$\delta_{\leq 1.25} \uparrow$
Dataset	Encoder		
SANPO-Synthetic-Train	Resnet-50 [16]	0.27	
SANPO-Real-Train	Resnet-50 [16]	0.45	

Table 2. **SANPO Baseline Performance.** Performance of panoptic segmentation and depth estimation methods trained on SANPO-Real-Train and SANPO-Synthetic-Train datasets.

Panoptic Segmentation : Kmax-DeepLab [50]			
Dataset	Encoder	mIoU \uparrow	PQ \uparrow
SANPO-Real-Train	Resnet-50 [16]	43.4	34.6
SANPO-Real-Train ‡	Resnet-50 [16]	42.7	34.6
SANPO-Real-Train	ConvNeXt-L [28]	46.0	38.4
SANPO-Real-Train ‡	ConvNeXt-L [28]	46.5	38.2

Table 3. **Accurate Machine Propagated Annotations.** Inclusion of machine propagated ground truth in the training of panoptic segmentation models does not compromise model performance. ‡: Human annotated GT only.

Synthetic to Real Domain Adaptation Table 4 demonstrates consistent improvements when pretraining on synthetic data before fine-tuning on real data (see rows marked with ->). Training on both synthetic and real data also yields better results, although the optimal mixture varies.

6. Applications

SANPO serves as the flagship training set for Project Guideline [15], a mobile application which uses SANPO-trained mobile-friendly depth estimation and semantic segmentation models to help people with low vision walk and run independently. The Project Guideline authors have already open-sourced their models trained on SANPO. [15]

Obstacle detection task SANPO focuses on depth estimation and panoptic segmentation because these are critical building blocks required by outdoor visual navigation tasks. This makes SANPO uniquely suited for these downstream navigation applications. To showcase this, we designed a simple on-device obstacle localization benchmark using SANPO-Real’s depth and panoptic labels. In this benchmark, we focus on three capabilities: (i) detecting walkable vs non-walkable surfaces, (ii) recognizing and detecting obstacles, (iii) determining ego person’s distance to the obstacles. These tasks are appropriate because tasks (ii) and (iii) need both segmentation and depth estimation, while (i)

Dataset	Encoder	mIoU \uparrow	PQ \uparrow
SANPO-Synthetic-Train	Resnet-50 [16]	14.6	9.6
SANPO-Synthetic-Train \rightarrow SANPO-Real-Train \ddagger	Resnet-50 [16]	44.1	34.6
SANPO-Synthetic-Train + SANPO-Real-Train 80% Synthetic \dagger	Resnet-50 [16]	40.7	31.2
SANPO-Synthetic-Train + SANPO-Real-Train 50% Synthetic \dagger	Resnet-50 [16]	43.0	34.6
SANPO-Synthetic-Train	ConvNeXt-L [28]	17.6	11.1
SANPO-Synthetic-Train \rightarrow SANPO-Real-Train \ddagger	ConvNeXt-L [28]	47.0	38.3
SANPO-Synthetic-Train + SANPO-Real-Train 80% Synthetic \dagger	ConvNeXt-L [28]	45.2	35.4
SANPO-Synthetic-Train + SANPO-Real-Train 50% Synthetic \dagger	ConvNeXt-L [28]	48.1	38.3

Table 4. **Synthetic Data Boosts Performance.** Incorporating synthetic data, either through pretraining or as a component of the training dataset, consistently improves performance. Kmax-DeepLab [50] is the method for all the rows. \rightarrow : Pretrained on synthetic and then fine-tuned on real data. $+$: Trained on combined real and synthetic data. \ddagger : Human annotated GT only.

Segmentation mIoU \uparrow		
safe for walking	not safe for walking	obstacles
83.4	64.5	85.9
Obstacles' Depth Estimation $\delta_{\leq 1.25} \uparrow$		
<10 meters	< 15 meters	<80 meters
0.27	0.25	0.20

Table 5. **On-device Navigation specific Segmentation and Obstacle Detection.**

mainly requires reliable segmentation. **Metrics.** For this task, we mapped SANPO labels to “safe for walking,” “not safe for walking,” and “obstacles” (Refer to A.6.1 in the supplementary material). For (i) and (ii), we report mIoU. For (iii), we report ≤ 1.25 of only obstacle classes, binning the metric at short range, medium range, and long range. **Baselines.** For semantic segmentation, we trained a quantized MobileNetV3 [17] with an input resolution of 512×512 . For depth estimation, we used a small MidasNet model [23] with an input resolution of 192×192 . Depth output is resized to 512×512 , with metrics reported at this resolution. These lightweight models run in real-time at 30FPS on Pixel 6 phones. See Table 5 for results.

7. Limitations and Future Work

SANPO focuses on outdoor environments, but it does not cover all possible navigation scenarios for the visually impaired. Limitations of SANPO include USA-centric geography, lack of indoor environments, and lack of nighttime data. Most comparable scene understanding datasets (KITTI [12], SideGuide [35], NYU [32], SCAND [20], MuSoHu [34],

etc.) are collected in a single geographic location. In comparison, SANPO, similar to Waymo Open [30], was collected in four regions across the USA: California (San Francisco and Mountain View), Colorado (Boulder), and New York City. This represents a geographically diverse blend of West Coast, Rocky Mountains, and Northeast environments in urban, suburban, and park settings. We chose these four regions in a single country because collecting data like SANPO is a very involved, costly, and manpower-intensive process and has to pass several state, city and local legal requirements. We excluded indoor environments because of legal and privacy considerations. For low-light and nighttime data, 10% of sessions in SANPO-Synthetic are rendered from nighttime environments. We kept this at 10% to prevent the domain similarity from diverging between SANPO-Real and SANPO-Synthetic. Extending our efforts to other countries, regions, and indoor environments, as well as including more nighttime data is something we will consider in the future. Additional synthetic-to-real experiments is future work as well.

8. Conclusion

This paper introduces SANPO, a large-scale egocentric video dataset that accelerates the development of computer vision-based assistive technologies. SANPO provides a comprehensive resource for researchers, offering diverse real and synthetic data alongside mobile-friendly, pre-trained models for semantic segmentation and depth estimation. We open-sourced both the dataset and models under the CC BY 4.0 license² to empower the CV community in building robust human egocentric navigation systems.

² <http://creativecommons.org/licenses/by/4.0>

References

- [1] Faruk Ahmed and Mohammed Yeasin. Optimization and evaluation of deep architectures for ambient awareness on a sidewalk. In *2017 International Joint Conference on Neural Networks (IJCNN)*, pages 2692–2697. IEEE, 2017. 2
- [2] Hangbo Bao, Li Dong, and Furu Wei. Beit: BERT pre-training of image transformers. *CoRR*, abs/2106.08254, 2021. 6
- [3] Shariq Farooq Bhat, Reiner Birkel, Diana Wofk, Peter Wonka, and Matthias Müller. Zoedepth: Zero-shot transfer by combining relative and metric depth, 2023. 5, 6
- [4] Rupert Bourne, Jaimie D Steinmetz, Seth Flaxman, Paul Svitil Briant, Hugh R Taylor, Serge Resnikoff, Robert James Casson, Amir Abdoli, Eman Abu-Gharbieh, Ashkan Afshin, et al. Trends in prevalence of blindness and distance and near vision impairment over 30 years: an analysis for the global burden of disease study. *The Lancet global health*, 9(2):e130–e143, 2021. 1
- [5] Gabriel J. Brostow, Julien Fauqueur, and Roberto Cipolla. Semantic object classes in video: A high-definition ground truth database. *Pattern Recognition Letters*, 30(2):88–97, 2009. Video-based Object and Event Analysis. 2, 13
- [6] Sergi Caelles, Jordi Pont-Tuset, Federico Perazzi, Alberto Montes, Kevis-Kokitsi Maninis, and Luc Van Gool. The 2019 davis challenge on vos: Unsupervised multi-object segmentation. *arXiv:1905.00737*, 2019. 2, 13
- [7] Holger Caesar, Varun Bankiti, Alex H. Lang, Sourabh Vora, Venice Erin Liong, Qiang Xu, Anush Krishnan, Yu Pan, Giancarlo Baldan, and Oscar Beijbom. nuscenes: A multimodal dataset for autonomous driving. *arXiv preprint arXiv:1903.11027*, 2019. 2, 13
- [8] Bowen Cheng, Ishan Misra, Alexander G. Schwing, Alexander Kirillov, and Rohit Girdhar. Masked-attention mask transformer for universal image segmentation. In *CVPR*, 2022. 17
- [9] Marius Cordts, Mohamed Omran, Sebastian Ramos, Timo Rehfeld, Markus Enzweiler, Rodrigo Benenson, Uwe Franke, Stefan Roth, and Bernt Schiele. The cityscapes dataset for semantic urban scene understanding. In *Proceedings of the IEEE Conference on Computer Vision and Pattern Recognition (CVPR)*, 2016. 2, 5, 6
- [10] Henghui Ding, Chang Liu, Shuting He, Xudong Jiang, Philip H. S. Torr, and Song Bai. Mose: A new dataset for video object segmentation in complex scenes, 2023. 15
- [11] Matteo Fabbri, Guillem Brasó, Gianluca Maugeri, Aljoša Ošep, Riccardo Gasparini, Orcun Cetintas, Simone Calderara, Laura Leal-Taixé, and Rita Cucchiara. Motsynth: How can synthetic data help pedestrian detection and tracking? In *International Conference on Computer Vision (ICCV)*, 2021. 2
- [12] Andreas Geiger, Philip Lenz, and Raquel Urtasun. Are we ready for autonomous driving? the kitti vision benchmark suite. In *Proceedings of the IEEE Conference on Computer Vision and Pattern Recognition (CVPR)*, 2012. 6, 8
- [13] Kristen Grauman, Andrew Westbury, Eugene Byrne, Zachary Chavis, Antonino Furnari, Rohit Girdhar, Jackson Hamburger, Hao Jiang, Miao Liu, Xingyu Liu, et al. Ego4d: Around the world in 3,000 hours of egocentric video. In *Proceedings of the IEEE/CVF Conference on Computer Vision and Pattern Recognition*, pages 18995–19012, 2022. 2
- [14] Vitor Guizilini, Rares Ambrus, Sudeep Pillai, Allan Raventos, and Adrien Gaidon. 3d packing for self-supervised monocular depth estimation. In *IEEE Conference on Computer Vision and Pattern Recognition (CVPR)*, 2020. 13
- [15] Dave Hawkey. Open sourcing project guideline: A platform for computer vision accessibility technology. Technical report. 7
- [16] Kaiming He, Xiangyu Zhang, Shaoqing Ren, and Jian Sun. Deep residual learning for image recognition. In *Proceedings of the IEEE conference on computer vision and pattern recognition*, pages 770–778, 2016. 6, 7, 8
- [17] Andrew Howard, Mark Sandler, Grace Chu, Liang-Chieh Chen, Bo Chen, Mingxing Tan, Weijun Wang, Yukun Zhu, Ruoming Pang, Vijay Vasudevan, Quoc V. Le, and Hartwig Adam. Searching for mobilenetv3, 2019. 8
- [18] Xinyu Huang, Xinjing Cheng, Qichuan Geng, Binbin Cao, Dingfu Zhou, Peng Wang, Yuanqing Lin, and Ruigang Yang. The apolloscape dataset for autonomous driving. *arXiv:1803.06184*, 2018. 13
- [19] Yue Kang, Hang Yin, and Christian Berger. Test your self-driving algorithm: An overview of publicly available driving datasets and virtual testing environments. *IEEE Transactions on Intelligent Vehicles*, 4(2):171–185, 2019. 2
- [20] Haresh Karnan, Anirudh Nair, Xuesu Xiao, Garrett Warnell, Sören Pirk, Alexander Toshev, Justin Hart, Joydeep Biswas, and Peter Stone. Socially compliant navigation dataset (scand): A large-scale dataset of demonstrations for social navigation. *IEEE Robotics and Automation Letters*, 7(4):11807–11814, 2022. 2, 8, 13
- [21] Alexander Kirillov, Eric Mintun, Nikhila Ravi, Hanzi Mao, Chloe Rolland, Laura Gustafson, Tete Xiao, Spencer Whitehead, Alexander C. Berg, Wan-Yen Lo, Piotr Dollár, and Ross Girshick. Segment anything, 2023. 5, 6
- [22] Bineeth Kuriakose, Raju Shrestha, and Frode Eika Sandnes. Tools and technologies for blind and visually impaired navigation support: a review. *IETE Technical Review*, 39(1):3–18, 2022. 1
- [23] Katrin Lasinger, René Ranftl, Konrad Schindler, and Vladlen Koltun. Towards robust monocular depth estimation: Mixing datasets for zero-shot cross-dataset transfer. *CoRR*, abs/1907.01341, 2019. 8
- [24] Jiankun Li, Peisen Wang, Pengfei Xiong, Tao Cai, Ziwei Yan, Lei Yang, Jiangyu Liu, Haoqiang Fan, and Shuaicheng Liu. Practical stereo matching via cascaded recurrent network with adaptive correlation, 2022. 2, 4
- [25] Zhenyu Li, Xuyang Wang, Xianming Liu, and Junjun Jiang. Binsformer: Revisiting adaptive bins for monocular depth estimation, 2022. 6, 7
- [26] Yiyi Liao, Jun Xie, and Andreas Geiger. KITTI-360: A novel dataset and benchmarks for urban scene understanding in 2d and 3d. *Pattern Analysis and Machine Intelligence (PAMI)*, 2022. 2, 13
- [27] Tsung-Yi Lin, Michael Maire, Serge Belongie, James Hays, Pietro Perona, Deva Ramanan, Piotr Dollár, and C Lawrence

- Zitnick. Microsoft coco: Common objects in context. In *Computer Vision—ECCV 2014: 13th European Conference, Zurich, Switzerland, September 6-12, 2014, Proceedings, Part V 13*, pages 740–755. Springer, 2014. [2](#), [13](#)
- [28] Zhuang Liu, Hanzi Mao, Chao-Yuan Wu, Christoph Feichtenhofer, Trevor Darrell, and Saining Xie. A convnet for the 2020s. *ieee*. In *CVF Conference on Computer Vision and Pattern Recognition (CVPR)*, volume 2, page 7, 2022. [6](#), [7](#), [8](#)
- [29] Ruiqing Mao, Jingyu Guo, Yukuan Jia, Yuxuan Sun, Sheng Zhou, and Zhisheng Niu. Dolphins: Dataset for collaborative perception enabled harmonious and interconnected self-driving. In *Proceedings of the Asian Conference on Computer Vision (ACCV)*, pages 4361–4377, December 2022. [2](#), [13](#)
- [30] Jieru Mei, Alex Zihao Zhu, Xinchun Yan, Hang Yan, Siyuan Qiao, Yukun Zhu, Liang-Chieh Chen, Henrik Kretschmar, and Dragomir Anguelov. Waymo open dataset: Panoramic video panoptic segmentation, 2022. [2](#), [8](#), [13](#)
- [31] Muhammad Shahroz Nadeem, Virginia NL Franqueira, Fatih Kurugollu, and Xiaojun Zhai. Wvd: A new synthetic dataset for video-based violence detection. In *Artificial Intelligence XXXVI: 39th SGAI International Conference on Artificial Intelligence, AI 2019, Cambridge, UK, December 17–19, 2019, Proceedings 39*, pages 158–164. Springer, 2019. [2](#)
- [32] Pushmeet Kohli Nathan Silberman, Derek Hoiem and Rob Fergus. Indoor segmentation and support inference from rgb-d images. In *ECCV*, 2012. [8](#)
- [33] Gerhard Neuhof, Tobias Ollmann, Samuel Rota Bulo, and Peter Kotschieder. The mapillary vistas dataset for semantic understanding of street scenes. In *Proceedings of the IEEE International Conference on Computer Vision (ICCV)*, Oct 2017. [2](#)
- [34] Duc M Nguyen, Mohammad Nazeri, Amirreza Payandeh, Aniket Datar, and Xuesu Xiao. Toward human-like social robot navigation: A large-scale, multi-modal, social human navigation dataset. *arXiv preprint arXiv:2303.14880*, 2023. [2](#), [8](#), [13](#)
- [35] Kibaek Park, Youngtaek Oh, Soomin Ham, Kyungdon Joo, Hyokyoung Kim, Hyoyoung Kum, and In So Kweon. Sideguide: a large-scale sidewalk dataset for guiding impaired people. In *2020 IEEE/RSJ International Conference on Intelligent Robots and Systems (IROS)*, pages 10022–10029, 2020. [2](#), [4](#), [8](#), [13](#)
- [36] Xingchao Peng, Ben Usman, Neela Kaushik, Dequan Wang, Judy Hoffman, and Kate Saenko. Visda: A synthetic-to-real benchmark for visual domain adaptation. In *Proceedings of the IEEE Conference on Computer Vision and Pattern Recognition Workshops*, pages 2021–2026, 2018. [4](#)
- [37] Federico Perazzi, Jordi Pont-Tuset, Brian McWilliams, Luc Van Gool, Markus Gross, and Alexander Sorkine-Hornung. A benchmark dataset and evaluation methodology for video object segmentation. In *Proceedings of the IEEE conference on computer vision and pattern recognition*, pages 724–732, 2016. [15](#)
- [38] Quang-Hieu Pham, Pierre Sevestre, Ramanpreet Singh Pahwa, Huijing Zhan, Chun Ho Pang, Yuda Chen, Armin Mustafa, Vijay Chandrasekhar, and Jie Lin. A*3d dataset: Towards autonomous driving in challenging environments. In *Proceedings of The International Conference in Robotics and Automation (ICRA)*, 2020. [2](#), [13](#)
- [39] Siyuan Qiao, Yukun Zhu, Hartwig Adam, Alan Yuille, and Liang-Chieh Chen. Vip-deeplab: Learning visual perception with depth-aware video panoptic segmentation. *arXiv preprint arXiv:2012.05258*, 2020. [2](#), [6](#), [13](#)
- [40] Arun V Reddy, Ketul Shah, William Paul, Rohita Mocharla, Judy Hoffman, Kapil D Katyal, Dinesh Manocha, Celso M de Melo, and Rama Chellappa. Synthetic-to-real domain adaptation for action recognition: A dataset and baseline performances. *arXiv preprint arXiv:2303.10280*, 2023. [4](#)
- [41] Stephan R Richter, Zeeshan Hayder, and Vladlen Koltun. Playing for benchmarks. In *Proceedings of the IEEE International Conference on Computer Vision (ICCV)*, pages 2213–2222, 2017. [2](#), [13](#)
- [42] Olga Russakovsky, Jia Deng, Hao Su, Jonathan Krause, Sanjeev Satheesh, Sean Ma, Zhiheng Huang, Andrej Karpathy, Aditya Khosla, Michael Bernstein, et al. Imagenet large scale visual recognition challenge. *International journal of computer vision*, 115:211–252, 2015. [17](#)
- [43] Konstantin Sofiiuk, Ilya A Petrov, and Anton Konushin. Reviving iterative training with mask guidance for interactive segmentation. In *2022 IEEE International Conference on Image Processing (ICIP)*, pages 3141–3145. IEEE, 2022. [5](#)
- [44] Mark Weber, Huiyu Wang, Siyuan Qiao, Jun Xie, Maxwell D. Collins, Yukun Zhu, Liangzhe Yuan, Dahun Kim, Qihang Yu, Daniel Cremers, Laura Leal-Taixe, Alan L. Yuille, Florian Schroff, Hartwig Adam, and Liang-Chieh Chen. DeepLab2: A TensorFlow Library for Deep Labeling. *arXiv: 2106.09748*, 2021. [17](#)
- [45] Benjamin Wilson, William Qi, Tanmay Agarwal, John Lambert, Jagjeet Singh, Siddhesh Khandelwal, Bowen Pan, Ratnesh Kumar, Andrew Hartnett, Jhony Kaesemodel Pontes, et al. Argoverse 2: Next generation datasets for self-driving perception and forecasting. *arXiv preprint arXiv:2301.00493*, 2023. [2](#), [13](#)
- [46] Ning Xu, Linjie Yang, Yuchen Fan, Dingcheng Yue, Yuchen Liang, Jianchao Yang, and Thomas Huang. Youtube-vos: A large-scale video object segmentation benchmark. *arXiv preprint arXiv:1809.03327*, 2018. [2](#), [13](#)
- [47] Kailun Yang, Luis M Bergasa, Eduardo Romera, and Kaiwei Wang. Robustifying semantic cognition of traversability across wearable rgb-depth cameras. *Applied optics*, 58(12):3141–3155, 2019. [2](#)
- [48] Lihe Yang, Bingyi Kang, Zilong Huang, Xiaogang Xu, Jiashi Feng, and Hengshuang Zhao. Depth anything: Unleashing the power of large-scale unlabeled data. *arXiv:2401.10891*, 2024. [5](#), [6](#)
- [49] Zongxin Yang, Yunchao Wei, and Yi Yang. Associating objects with transformers for video object segmentation. In *Advances in Neural Information Processing Systems (NeurIPS)*, 2021. [15](#), [16](#)
- [50] Qihang Yu, Huiyu Wang, Siyuan Qiao, Maxwell Collins, Yukun Zhu, Hartwig Adam, Alan Yuille, and Liang-Chieh Chen. kmax-deeplab: k-means mask transformer, 2023. [5](#), [6](#), [7](#), [8](#)

A. Appendix

A.1. Data Collection

A.1.1 Rig

To accommodate SANPO-Real’s multi stereo camera requirements we designed a specialized data collection rig. This rig prioritizes hardware integration, reliable GPU cooling, and comfort for the wearer. Our setup involves volunteers wearing head and chest mounted ZED cameras (ZED-M and ZED-2i, respectively), with supporting hardware in a backpack. We also developed a mobile app for visualization and to control the data collection. Figure 9 shows the data collection system in action.



Figure 9. SANPO-Real Data Collection Rig.

A.2. Dataset

A.2.1 SANPO-Synthetic Reproducibility and rendering environment.

We created SANPO-Synthetic through our collaboration with a third party, Parallel Domain. If other researchers wish to reproduce these environments with other tools (NVIDIA Omniverse, Unreal, Unity, etc), we would welcome that. To aid reproducibility, here are detailed specifications for SANPO-Synthetic’s virtual rendering environment.

All % are at session level.

1. Scene types : Urban environments only.

2. Camera Type : Zed 2i

(a) Image width: 2208

(b) Image height: 1242

(c) fx: 1914.203

(d) fy: 1914.203

(e) cx: 1074.4403

(f) cy: 655.79846

(g) camera matrix:

$$\begin{pmatrix} 1914.203 & 0 & 1074.4403 \\ 0 & 1914.203 & 655.79846 \\ 0 & 0 & 1 \end{pmatrix}$$

(h) stereo transform (between left/right cameras):

$$\begin{pmatrix} 1 & 0 & 0 & 119.96817 \\ 0 & 1 & 0 & 0 \\ 0 & 0 & 1 & 0 \\ 0 & 0 & 0 & 1 \end{pmatrix}$$

3. Camera Type : Zed Mini

(a) image_width: 2208

(b) image_height: 1242

(c) fx: 1376.4702

(d) fy: 1376.4702

(e) cx: 1112.7797

(f) cy: 599.8397

(g) camera matrix:

$$\begin{pmatrix} 1376.4702 & 0 & 1112.7797 \\ 0 & 1376.4702 & 599.8397 \\ 0 & 0 & 1 \end{pmatrix}$$

(h) stereo transform (between left/right cameras):

$$\begin{pmatrix} 1 & 0 & 0 & 62.944813 \\ 0 & 1 & 0 & 0 \\ 0 & 0 & 1 & 0 \\ 0 & 0 & 0 & 1 \end{pmatrix}$$

4. Camera Positions

(a) Zed 2i on chest.

(b) Zed mini just above head.

(c) Both with natural tilt variations.

(d) 50% of sessions from each position.

5. FPS (Frames per second)

(a) 60% at 5 FPS.

(b) 20% at 14.28 FPS.

(c) 20% at 33.33 FPS.

6. Ground truth annotations

(a) Panoptic segmentation mask.

(b) Metric depth map.

7. Lighting and Weather

(a) 70% well lit sunny

(b) 10% are at dawn/dusk with the sun low in the horizon

(c) 10% are dark/nighttime

(d) 5% have fog

- (e) 5% have rain
8. Obstacles
- (a) Garbage can
 - i. 50% One per street block.
 - ii. 30% two garbage cans. E.g: One normal and one recycle.
 - iii. 20% no garbage can.
 - (b) Trash bags
 - i. 50% None
 - ii. 40% 1-2
 - iii. 10% ≥ 5
 - (c) Bike racks : One per street block.
 - (d) Mailbox
 - i. 60% one per street block.
 - ii. 20% two adjacent mailboxes per street block.
 - iii. 20% None.
 - (e) Fire Hydrant
 - i. 80% One per street block.
 - ii. 20% None.
 - (f) Construction cones : As provided by the rendering scene map.
9. Road Vehicle : Low, mid and high is the setting in the rendering engine.
- (a) 20% None
 - (b) 30% low
 - (c) 30% mid
 - (d) 20% high
10. Pedestrians
- (a) 10 \geq per street block (50%)
 - (b) 5 \geq per street block (30%)
 - (c) < 3 per street block (20%)
 - (d) 20% very close to the ego person.
11. Trees on sidewalk
- (a) 60% high density.
 - (b) 20% low density.
 - (c) 20% no trees on the sidewalk.
12. Other naturally occurring things like curbs, dips, cross-walks, parking meters, traffic signs and lights, fences, plants, hedges etc.. will be included as provided by the rendering scene map.
13. Not Supported
- (a) Bike paths.
 - (b) Riders on sidewalk.
 - (c) Foliage and seasonal color changes of leaves.

A.2.2 Dataset Comparison

While many outdoor video datasets exist for tasks like robot navigation, autonomous driving, and video segmentation (see Table 6), SANPO fills a crucial gap. To our knowledge, it is the only dataset providing both real and synthetic data with panoptic labels and depth maps specifically designed for human-centric egocentric navigation research.

Figure 10 provides a visual comparison between SANPO-Real and SANPO-Synthetic.



Figure 10. **SANPO Synthetic vs real.** A sample of SANPO-Real and SANPO-Synthetic data. *How quickly can you tell which of these images is synthetic?* Answer key in base64: `'c3ludGg6IEFCRUZILCByZWFsOiBDREc='`

A.2.3 Additional Statistics

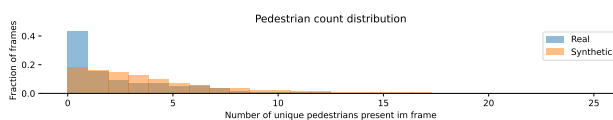


Figure 11. **Distribution of pedestrians** in SANPO-Real and SANPO-Synthetic. SANPO-Real frequently features images with no pedestrians, but pedestrians appear in almost all frames of SANPO-Synthetic, and in greater quantities.

Pedestrian density

Additional Attributes of SANPO-Synthetic's Segmentation Annotations

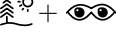
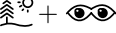
- Instance Density: Over half of the frames have ≥ 60 unique instances, with a sixth having ≥ 150 .
- Small Objects: 80% of object masks have less than 32^2 pixels, significantly more than SANPO-Real (8.1%).

A.3. Data Annotation

A.3.1 Session Attributes

Each real session is annotated with the following high level attributes.

1. Human Traffic
 - (a) Low
 - (b) Moderate

Dataset	Domain	Environment	# Frames	# Seg Masks	# Depth Maps
SCAND [20]			~522 minutes		~522 minutes
MuSoHu [34]			~600 minutes		~600 minutes
Playing for Benchmark (Synthetic) [41]			250K	250K (Dense)	
Cityscapes-DVPS [39]			3K	3K (Dense)	3K (Dense)
KITTI-360 [26]			320K	2x78K (Dense)	2x78K (Dense)
Panoptic-nuScenes [7]			1.4M	40K (Dense)	
Waymo Open Dataset -Panoramic [30]			390K	100K	
A*3D [38]			39K	39K (3D BBox)	
ApolloScape-SceneParsing [18]			140K	140K (Dense)	140K (Dense)
DDAD [14]			21K		21K (Dense)
DOLPHINS (Synthetic) [29]			42K	42K (3D BBox)	
Argoverse2 Sensor Data [45]			1000 (Videos)	3D BBox	
CamVid [5]			5 (Videos)	700 (Dense)	
MS-COCO [27]	O.D.S		328K	328K	
Youtube-VOS [46]	V.O.S.		~20K	~4K (Sparse)	
DAVIS-2017 [6]	V.O.S.		10K	10K (Sparse)	
SideGuide [35]			2x180K, 312K	100K (Sparse)	180K (Dense)
SANPO-Real (ours)			2x617K	112K (Dense)	617K (Dense)
SANPO-Synthetic (ours)			113K	113K (Dense)	113K (Dense)

 : Robot Navigation,  : Self-Driving,  : Egocentric Navigation,
O.D.S: Object Detection & Segmentation, V.O.S: Video Object Segmentation
 : Indoor,  : Outdoor,  Stereo

Table 6. **Dataset Comparison.** SANPO is a unique video dataset designed to address a gap in current offerings. Unlike existing datasets focused on self-driving vehicles or general video object segmentation (VOS), SANPO targets the specific challenges of egocentric human navigation. SANPO is a large-scale, challenging, and diverse dataset. It offers both real and synthetic data, with multi-view stereo data included in the real component.

- (c) Heavy
- 2. Vehicular Traffic
 - (a) Low
 - (b) Moderate
 - (c) Heavy
- 3. Animal Traffic
 - (a) Low
 - (b) Moderate
 - (c) Heavy
- 4. Number of Obstacles
 - (a) Low
 - (b) Moderate
 - (c) Heavy
- 5. Environment Type
 - (a) Urban
 - (b) Suburban
 - (c) Rural
 - (d) Park
 - (e) Road Junction
 - (f) Open Terrain
 - (g) Open Space
 - (h) Indoor
- 6. Weather Condition
 - (a) Sunny
 - (b) Cloudy
 - (c) Rainy
 - (d) Snowy
- 7. Visibility
 - (a) High
 - (b) Medium
 - (c) Low
- 8. Motion Type
 - (a) Walking
 - (b) Jogging
 - (c) Running
- 9. Elevation Change
 - (a) Flat

- (b) Uphill
- (c) Downhill
- (d) Stairs
- 10. Ground Appearances
 - (a) Light Gray
 - (b) Dark Gray
 - (c) Pavers
 - (d) Color
 - (e) Terrain
 - (f) Gravel
 - (g) Sand
- 11. Motion Blur
 - (a) Low
 - (b) Medium
 - (c) High
- 12. Rare Events

A.3.2 SANPO Taxonomy

SANPO taxonomy labels with *stuff* or *thing* distinction.

- 0. unlabeled → stuff
- 1. road → stuff
- 2. curb → stuff
- 3. sidewalk → stuff
- 4. guard rail/road barrier → stuff
- 5. crosswalk → thing
- 6. paved trail → stuff
- 7. building → stuff
- 8. wall/fence → stuff
- 9. hand rail → stuff
- 10. opening-door → thing
- 11. opening-gate → thing
- 12. pedestrian → thing
- 13. rider → thing
- 14. animal → thing
- 15. stairs → thing

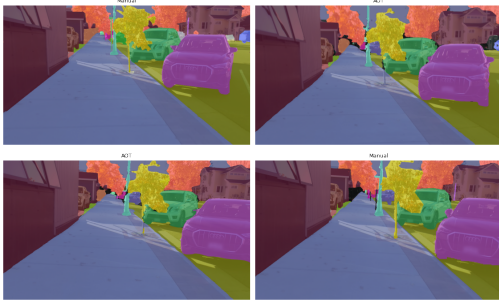


Figure 12. **Temporally Consistent Segmentation Annotation.** Our annotation process ensures temporal consistency across both human-annotated and machine-propagated masks. Compare the first and last columns of the figure to see this consistency. Most propagated masks are accurate, with occasional failures for thin objects like trees (yellow) and poles (cyan).

This process resulted in 18,787 human-annotated frames and 93,981 machine-propagated frames.

Evaluating AOT-Based Propagation Accuracy To evaluate the accuracy of AOT-based propagation for segmentation annotations, we performed the following analysis. We considered human-annotated frames (0-6-12-...), propagated segmentation masks to every other frame (6-18-...) using AOT, and compared these propagated masks to the corresponding human-annotated ground truth (GT) to calculate a propagation score. Since the motion gap between these frames is significant, this method provides a conservative estimate (lower bound) of the propagation error. In accordance with the video object segmentation (VOS) literature [10, 37, 49], we used region similarity J and contour accuracy F as evaluation metrics. The mean $J&F$ score for SANPO-Real is 0.892, demonstrating a strong lower bound on the accuracy of machine-propagated masks.

Detailed and Accurate Segmentation Annotation Our dataset captures rich details, including high-quality semantic masks for even the smallest objects (see Fig. 13 for examples).

A.4. Benchmarks

A.4.1 Zero Shot Evaluation

Cityscapes-19 -> SANPO Mapping

To ensure a fair comparison, we map Cityscapes-19 labels to SANPO labels wherever possible. Below mapping from Cityscapes-19 to SANPO taxonomy:

1. road → road
2. sidewalk → sidewalk
3. building → building
4. wall → wall/fence

³ We experimented with various combinations to refine this approach.

16. water body → stuff
17. other walkable surface → stuff
18. inaccessible surface → stuff
19. railway track → stuff
20. obstacle → thing
21. vehicle → thing
22. traffic sign → thing
23. traffic light → thing
24. pole → thing
25. bus stop → thing
26. bike rack → thing
27. sky → stuff
28. tree → thing
29. vegetation → stuff
30. terrain → stuff

A.3.3 Segmentation Annotation Process

In this section we describe the segmentation annotation process for SANPO-Real. We divide each video into 30-second sub-videos (note: most videos are only 30 seconds long, resulting in a single sub-video), then we annotate every sixth frame (0-6-12-...), for a total of 90 frames per sub-video. To enhance efficiency and accuracy of human annotation, we employ two key techniques:

- Cascaded Annotation: To manage our extensive taxonomy, we divide all labels into five mutually exclusive subsets containing commonly co-occurring labels. Each sub-video is annotated in a temporally consistent manner across these subsets in a carefully determined optimal order³. When annotating a subset, previously annotated regions are frozen and displayed to the annotator, thus increasing their speed and improving boundary precision. The final subset includes all labels, ensuring that any regions missed in previous subsets are annotated.
- AOT based Propagation: We leverage AOT [49] to propagate masks from human-annotated frames to the intermediate unannotated frames. We track whether each frame is human-annotated or machine-propagated, and this information is included alongside the provided annotations. Figure 12 visually demonstrates this process, showing human-annotated frames and their machine-propagated counterparts.



Figure 13. SANPO’s detailed annotation include masks for even the smallest objects (highlighted in purple, right column).

- | | |
|----------------------------------|--------------------------|
| 5. fence → wall/fence | 12. person → pedestrian |
| 6. pole → pole | 13. rider → rider |
| 7. traffic light → traffic light | 14. car → vehicle |
| 8. traffic sign → traffic sign | 15. truck → vehicle |
| 9. vegetation → vegetation | 16. bus → vehicle |
| 10. terrain → terrain | 17. train → vehicle |
| 11. sky → sky | 18. motorcycle → vehicle |
| | 19. bicycle → vehicle |

For all SANPO labels without an appropriate mapping from Cityscapes-19, we treat the corresponding pixels as unlabeled and exclude them from the mIoU metric computation in the zero-shot semantic segmentation evaluation. The following SANPO labels were excluded:

- | | |
|----------------------------|----------------------------|
| 1. curb | 10. water body |
| 2. guard rail/road barrier | 11. other walkable surface |
| 3. crosswalk | 12. inaccessible surface |
| 4. paved trail | 13. railway track |
| 5. hand rail | 14. obstacle |
| 6. opening-door | 15. bus stop |
| 7. opening-gate | 16. bike rack |
| 8. animal | 17. tree |
| 9. stairs | |

Zero-shot Mask2Former Evaluation

We also evaluated the Mask2Former Swin-L model [8] in the zero-shot setting. Despite its strong performance on Cityscapes (mIoU 0.833), it achieved lower scores on SANPO-Real (0.417) and SANPO-Synthetic (0.476). Fig. 14 offers a qualitative assessment on SANPO samples and Table 7 provides a class-wise mIoU breakdown.

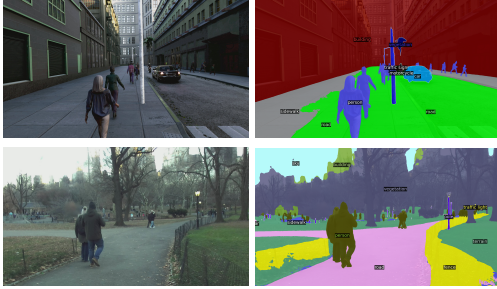


Figure 14. **Highlight on Domain Gap.** Egocentric navigation models must accurately differentiate between road (a not safe to walk surface) and sidewalk (a safe to walk surface). Mask2Former trained on Cityscapes dataset, similar to the Kmax-Deeplab models, struggles with this distinction on SANPO samples (top: synthetic, bottom: real). This, along with Table 1, underscores the limited transferability of such datasets to human-centric navigation tasks. This visualization is generated using the Mask2Former tool [8].

A.4.2 SANPO Benchmark

To ensure fairness and reproducibility, we maintained the following training setup:

1. **Encoder Pretraining:** All encoders pretrained on ImageNet [42].
2. **Datasets Used:** Only SANPO train sets.
3. **Resizing:** Data resized to 1089x1921 (height x width), padding used to maintain aspect ratio.
4. **Hyperparameters:** Standard values as defined in [44].
5. **Training Budget:** 60,000 steps with a batch size of 32 (doubled for Synthetic-to-Real domain adaptation fine-tuning experiments (-> and + rows in Table 4)). Approximate epochs for reference:
 - Cityscapes Panoptic Segmentation: 645
 - SANPO-Real Panoptic Segmentation: 21
 - SANPO-Real (Human GT Only) Panoptic Segmentation: 129
 - SANPO-Synthetic Panoptic Segmentation and Depth Estimation: 21
 - SANPO-Real Depth Estimation: 4

Mapped SANPO Label	mIoU	
	SANPO-Real	SANPO-Synthetic
road	0.255	0.407
sidewalk	0.120	0.262
building	0.642	0.934
wall/fence	0.448	0.087
pedestrian	0.679	0.878
rider	0.271	0.247
vehicle	0.658	0.817
traffic sign	0.212	0.240
traffic light	0.127	0.344
pole	0.310	0.586
sky	0.658	0.919
vegetation	0.654	0.303
terrain	0.394	0.166
Average	0.417	0.476

Table 7. **Mask2Former Zero-Shot Evaluation:** Per label breakdown of mIoU on the Mask2Former (Cityscapes) zero-shot experiment.

A.5. SANPO Dense Prediction Qualitative Examples

We show some example images in Fig. 15, as well as ground truth and predicted segmentation maps from kMax-Deeplab and ground truth and predicted depth maps from Binsformer.

A.6. Application

A.6.1 SANPO -> Accessibility Mapping

"safe to walk" (e.g. sidewalk) and "not safe to walk" (e.g. road, which is for vehicles) are ground surfaces.

1. unlabeled → not safe to walk
2. road → not safe to walk
3. curb → not safe to walk
4. sidewalk → safe to walk
5. guard rail/road barrier → obstacle
6. crosswalk → safe to walk
7. paved trail → safe to walk
8. building → obstacles
9. wall/fence → obstacles
10. hand rail → obstacles
11. opening-door → obstacles
12. opening-gate → obstacles

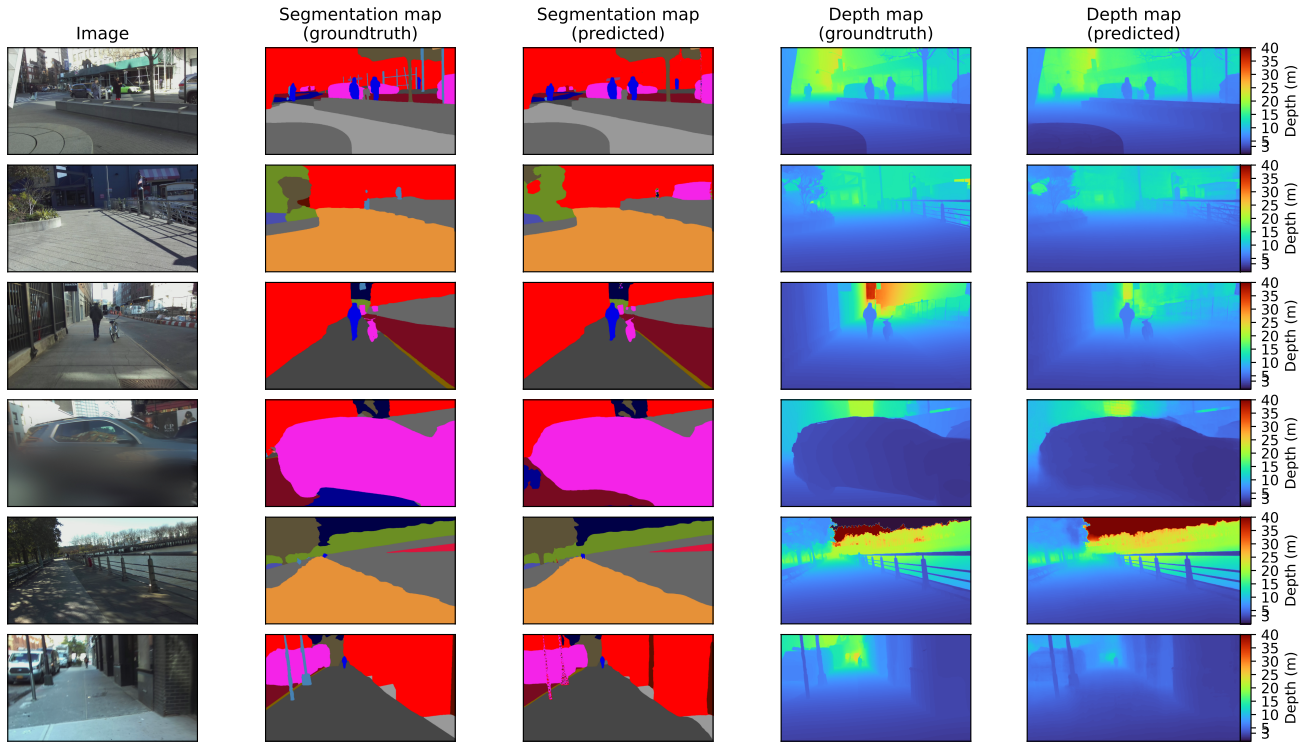


Figure 15. **Qualitative examples on SANPO.** Showing left to right: image, groundtruth & predicted segmentation maps, and groundtruth & predicted metric depth maps.

- | | |
|---|----------------------------|
| 13. pedestrian → obstacles | 29. tree → obstacles |
| 14. rider → obstacles | 30. vegetation → obstacles |
| 15. animal → obstacles | 31. terrain → safe to walk |
| 16. stairs → safe to walk | |
| 17. water body → not safe to walk | |
| 18. other walkable surface → safe to walk | |
| 19. inaccessible surface → not safe to walk | |
| 20. railway track → not safe to walk | |
| 21. obstacle → obstacles | |
| 22. vehicle → obstacles | |
| 23. traffic sign → obstacles | |
| 24. traffic light → obstacles | |
| 25. pole → obstacles | |
| 26. bus stop → obstacles | |
| 27. bike rack → obstacles | |
| 28. sky → not safe to walk | |